New aspects in assessment of changes in width of subarachnoid space with near-infrared transillumination/backscattering sounding, part 2: clinical verification in the patient

Andrzej F. Frydrychowski
Medical University of Gdańsk
Department of Physiology
ul. Dębinki 1
80-211 Gdańsk, Poland

Jerzy Pluciński
Gdańsk University of Technology
Faculty of Electronics Telecommunications, and Informatics
Department of Optoelectronics
ul. Narutowicza 11/12
80-952 Gdańsk, Poland
E-mail: pluc@eti.pg.gda.pl

Abstract. The study presents comparison of near-infrared light propagation and near-infrared backscattered radiation power, as simulated with numerical modeling and measured live in a patient in clinical conditions with the use of the near-infrared transillumination/backscattering sounding (NIR-T/BSS) technique. A unique chance for such precise comparative analysis was available to us in a clinical case of a female patient with scalp removed from one half of the head due to injury. The analysis performed indicates that the difference between the intensity of the signals in numerical modeling and live measurements is less than 4 dB. Analysis of the theoretical model also provides hints on the positioning of the two detectors relative to the source of radiation. Correctness of these predicted values is confirmed in practical application, when changes of signals received by the detectors are recorded, along with changes of the width of the subarachnoid space. What is more, the power distribution of the spectrum of near-infrared backscattered radiation returning to the detectors is confirmed in the real recording in the patient. An abridged description of the new method of NIR-T/BSS is presented. [DOI: 10.1117/1.2753756]

Keywords: transillumination; near-infrared radiation; optical measurement; head tissue propagation; subarachnoid space.

Paper 06269 received Sep. 26, 2006; accepted for publication Feb. 20, 2007; published online Jul. 13, 2007.

1 Introduction

Elaboration of a theoretical model[1,2] and measurement system for a new, noninvasive method of recording changes of the width of subarachnoid space (SAS)[3] enabled recordings in a number of clinical situations. The risk included development of elevated intracranial pressure, until now detectable and monitored only with invasive diagnostic techniques. As this method is relatively new, recordings are still needed to confirm the correctness of the theoretical assumptions and foundations of the method, as well as its suitability for clinical applications.

We decided to verify the results of numerical modeling of propagation of near-infrared (NIR) radiation within different anatomical layers and sites of the head different distances from the source, presented in the first part of this study. Real live recordings were done with a dedicated data acquisition and processing system, specialized for this technique. A unique and extremely valuable chance for such verification became available to us when we were allowed to perform the necessary measurements in a female patient who lost the scalp from exactly half of her head as a result of being severely battered. In these conditions it became possible to make recordings of signals carried by NIR radiation within and through different anatomical layers of the head, both with scalp included (detector placed on the surface of the skin) and with scalp excluded (detector placed directly on the surface of the skull bone).

The recordings and measurements in the patient were made with the use of a new and noninvasive method of near-infrared transillumination, explained in detail in earlier publications.[3–11] In this study we provide only an abridged description of the method for easy understanding of the method and the results obtained. In the method of NIR transillumination, application of an appropriate signal processing algorithm, consisting of division of the signal from the distal detector (DD) over that from the proximal detector (PD), yields a so-called transillumination quotient (TQ). This enables near-total elimination of the modulatory influence of cutaneous pulsatile blood flow on the recorded signals and TQ, thus providing insight into the intracranial phenomena affecting NIR propagation within the SAS. We have used only part of the capacity of this method, namely that of recording the power of NIR-backscattered radiation (NIR-BSR) at particular separate detectors (the PD and DD), positioned at dif-

Address all correspondence to Jerzy Pluciński, Dept. of Optoelectronics, Faculty of Elec. Telecom., & Informatics, Gdańsk University of Technology, Narutowicza 11/12, Gdańsk, PL 80-952 Poland

1083-3668/2007/12(4)/044016/8/$25.00 © 2007 SPIE

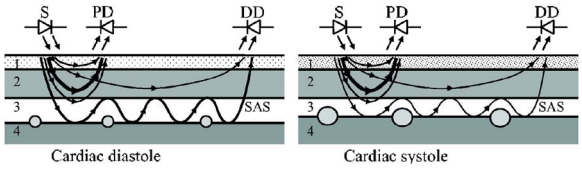

Fig. 1 A simplified diagram illustrating the influence of heart-pump-induced pulsatile changes affecting NIR propagation within the tissues of the head: 1. skin (dot density used as a proportional indicator of blood amount within the skin layer during particular phases of cardiac cycle), 2. skull bone, 3. SAS (adherent to the bone lined with the dura is the arachnoid, space beneath the arachnoid contains water-clear cerebrospinal fluid and blood vessels on the surface of the brain), 4. surface of the brain covered with the pia, adherent to brain surface and embedded within brain sulci and fissures are cerebral arteries and arterioles, as well as smaller diameter vessels in the form of a meshwork. Lines with arrows were used to show propagation of NIR in a proportional manner—thick line for a greater amount of radiation propagated, thinner line for a smaller amount of radiation propagated. S is the source, PD is the proximal detector, and DD is the distal detector.

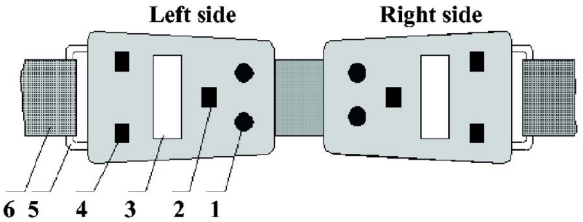

Fig. 2 Diagram of a set of detectors for the left and right sides of the head (inner aspect), which is placed directly on the surface of the skin. 1. Emitting diodes (source), 2. proximal detector, 3. conductive rubber band acting as ground lead for the module, 4. distal detectors, 5. mount frame, and 6. one-size-fits-all elastic ribbon.

ferent distances from the source of radiation. For further refinement of the algorithm for the elimination of the influence of pulsatile blood flow in the skin, it is necessary to design and assemble the source-detector module in line with the guidelines derived from the theoretical numerical model, and then rightly interpret the recordings obtained. Verification of the theoretical model is based on comparison of the experimental data obtained in live recordings from human subjects with the output data of the numerical model.

2 Abridged Description of the Method of Near-Infrared Transillumination

The method of monitoring instantaneous changes of the width of the subarachnoid space, employing NIR radiation and original solutions for the source-detector module and a dedicated hardware-software system for the acquisition and analysis of the received NIR signals, received the name of near-infrared transillumination/backscattering sounding (NIR-T/BSS). Such a name appears to be most appropriate, considering the factual measurement of the intensity of the radiation propagated "back" to the detectors, after its multiple reflections, and scattering within the tissues of the head it penetrates on its way. These elements make up the method that is a form of sounding of the instantaneous changes of the width of the biological optical duct formed by the SAS. A schematic diagram for the propagation of NIR to particular detectors (the PD and DD) in the phases of cardiac diastole and systole is shown in Fig. 1.[11] On its way from the source to the detectors, NIR becomes modulated within two propagation media: during passage through the skin and while propagating within the SAS. Modulation within the skull bone should be neglected, because—for a given individual—NIR attenuation by the bone remains constant. At its passage through the scalp, NIR receives pulsatile modulation related to heart-induced pulsatile changes of blood content in this layer: the amount of blood in the scalp increases synchronously with heart systole, and decreases with heart diastole. Our earlier analysis[3] revealed that blood attenuates NIR propagation very strongly, which implies that NIR attenuation increases with increased blood content in the scalp and decreases with decreased amount of blood in the scalp. In the phase of systole, when the amount of blood in the scalp increases, we should then expect increased attenuation of NIR penetrating the scalp and decreased amount of radiation reaching the detectors. During heart diastole—when filling of the blood vessels with blood decreases—NIR attenuation in the scalp should be decreased, thus allowing for more radiation to reach the detectors. The other site where NIR becomes modulated is the SAS. Intracranial pulsation of cerebrovascular origin causes oscillations of the width of the SAS dependent and synchronous with the changes in the filling of the intracranial arterial blood vessels in the cardiac cycle. Increased filling in the systolic phase results in a decrease of the width of the SAS optical duct, which in turn causes a decrease in the amount of radiation propagated from the source to the detectors. Noteworthy is the synchronous and synergistic effect on the amount of radiation received by the PD and DD of the oscillations of both blood filling of the vessels of the scalp and the width of the SAS. Recording of the NIR signals was done with the use of a special NIR-T/BSS source-detector module of our own design.

The construction of the source-detector module is based on the knowledge acquired from the theoretical model, and particularly on the conclusion that successful recording and measurements of the NIR signals requires and depends on very specific distances of the two detectors from the source of radiation. On the basis of the results of numerical modeling, we decided that the PD distance from the source should be 7 mm, while the DD should be positioned at a distance of 28 mm from the source (data for the detectors used in human subjects). Such a set of detectors for the right and left sides of the head is presented in Fig. 2. Inserted between the detectors is a conductive rubber strip, which is connected with the ground (zero) lead of the device. It is designed to enable connection between the patient and the grounding conductor of the device, so that the effect of the electric power network-induced noise on the signals from the detectors can be decreased. A one-size-fits-all elastic ribbon is attached to the sides of the modules via a mount frame. For the source of NIR, we used light-emitting diodes (LEDs) (type TSMF3700 by Vishay Semiconductors), emitting impulses of near-infrared radiation of wavelength 870 nm, which has been proved to easily penetrate tissues and be almost completely insensitive to changes in hemoglobin oxygen saturation.[12–15] A single NIR-T/BSS source-detector module, for one side of the head, is composed

of two LEDs, which constitute the source and receiving photodiodes (type TEMD5000 by Vishay Semiconductors), which act as NIR detectors: the proximal diode was positioned 7 mm away from the source, constituting the proximal photodiode (PD), and a set of two distal photodiodes 28 mm from the source, which collectively constituted the DD. During measurements, two identical NIR-T/BSS source-detector modules are used and placed symmetrically on the forehead, one for each side of the head. On its route from the source to the detectors (the PD and DD), NIR radiation crosses and propagates within blood supplied skin (scalp), skull bone, subarachnoid space, and then again through skull bone and skin, but in the reverse direction.

Next, we present an explanation of the reasoning behind the mathematical illustration of this NIR propagation sequence. Let us express the waveforms of intensities of the NIR signals reaching the detectors in a qualitative manner. If we assign i_S to the intensity of the radiation emitted by the NIR source and consider the fact that in a multilayer structure, the overall outcome transmittance coefficient is a product of the transmittance coefficients for particular layers, then we arrive at the following formula:

For the intensity at the proximal detector $i_{PD}(t)$:

$$\begin{aligned} i_{PD}(t) = [&\alpha_{\text{skin S-PD}}(t) + \alpha_{\text{skin S}}(t) \cdot \alpha_{\text{bone S-PD}}(t) \cdot \alpha_{\text{skin PD}}(t) \\ &+ \alpha_{\text{skin S}}(t) \cdot \alpha_{\text{bone S}}(t) \cdot \alpha_{\text{SAS S-PD}}(t) \cdot \alpha_{\text{bone PD}}(t) \\ &\cdot \alpha_{\text{skin PD}}(t) + \alpha_{\text{skin S}}(t) \cdot \alpha_{\text{bone S}}(t) \cdot \alpha_{\text{SAS S}}(t) \\ &\cdot \alpha_{\text{brain S-PD}}(t) \cdot \alpha_{\text{SAS PD}}(t) \cdot \alpha_{\text{bone PD}}(t) \\ &\cdot \alpha_{\text{skin PD}}(t)] \cdot i_S, \end{aligned} \tag{1}$$

where t is time; α is the transmission coefficient; indexes "skin," "bone," "SAS," and "brain" mean that transmission are in skin, bone, SAS, and brain, respectively; "S," "PD," and "DD" mean transverse transmission under the source, PD, and DD, respectively; and S-PD and S-DD mean longitudinal transmission between the source and proximal or distal detectors, respectively.

We can assume here that the first, third, and fourth components are very low compared to the second component of $i_{PD}(t)$, which can be explained with: 1. proximal detector-source distance exceeding the thickness of skin layer, 2. the results of the experiment with scalp compression between the NIR source and the PD, when no changes of $i_{PD}(t)$ were observed, and 3. $\alpha_{\text{brain S-PD}}(t)$ represents very low transmittance of the brain for near-infrared radiation.

Considering the previous, we receive:

$$i_{PD}(t) \cong \alpha_{\text{skin S}}(t) \cdot \alpha_{\text{bone S-PD}}(t) \cdot \alpha_{\text{skin PD}}(t) \cdot i_S. \tag{2}$$

Likewise, for the distal detector $i_{DD}(t)$:

$$\begin{aligned} i_{DD}(t) = [&\alpha_{\text{skin S-DD}}(t) + \alpha_{\text{skin S}}(t) \cdot \alpha_{\text{bone S-DD}}(t) \cdot \alpha_{\text{skin DD}}(t) \\ &+ \alpha_{\text{skin S}}(t) \cdot \alpha_{\text{bone S}}(t) \cdot \alpha_{\text{SAS S-DD}}(t) \cdot \alpha_{\text{bone DD}}(t) \\ &\cdot \alpha_{\text{skin DD}}(t) + \alpha_{\text{skin S}}(t) \cdot \alpha_{\text{bone S}}(t) \cdot \alpha_{\text{SAS S}}(t) \\ &\cdot \alpha_{\text{brain S-DD}}(t) \cdot \alpha_{\text{SAS DD}}(t) \cdot \alpha_{\text{bone DD}}(t) \\ &\cdot \alpha_{\text{skin DD}}(t)] \cdot i_S. \end{aligned} \tag{3}$$

Contrary to Eq. (1), we can assume that in Eq. (3) the first and fourth components are very low compared to the second and third components of $i_{DD}(t)$. Considering the previous, we receive:

$$\begin{aligned} i_{DD}(t) \cong &\alpha_{\text{skin S}}(t) \cdot \alpha_{\text{bone S-DD}}(t) \cdot \alpha_{\text{skin DD}}(t) \\ &+ \alpha_{\text{skin S}}(t) \cdot \alpha_{\text{bone S}}(t) \cdot \alpha_{\text{SAS S-DD}}(t) \\ &\cdot \alpha_{\text{bone DD}}(t) \cdot \alpha_{\text{skin DD}}(t) \cdot i_S. \end{aligned} \tag{4}$$

Given the previous, we arrive at the following formula for the quotient of transillumination signals received by the distal and proximal detectors $q(t)$:

$$q(t) = \frac{i_{DD}(t)}{i_{PD}(t)} \cong \frac{[\alpha_{\text{skin S}}(t) \cdot \alpha_{\text{bone S-DD}}(t) \cdot \alpha_{\text{skin DD}}(t) + \alpha_{\text{skin S}}(t) \cdot \alpha_{\text{bone S}}(t) \cdot \alpha_{\text{SASS-DD}}(t) \cdot \alpha_{\text{bone DD}}(t) \cdot \alpha_{\text{skin DD}}(t)] \cdot i_S}{\alpha_{\text{skin S}}(t) \cdot \alpha_{\text{bone S-PD}}(t) \cdot \alpha_{\text{skin PD}}(t) \cdot i_S}. \tag{5}$$

Assuming that $\alpha_{\text{bone S-PD}}(t)$, $\alpha_{\text{bone S-DD}}(t)$, $\alpha_{\text{bone PD}}(t)$, and $\alpha_{\text{bone DD}}(t)$ are not practically dependent on time (as mentioned before, modulation within skull bone should be neglected), and

$$\alpha_{\text{skin PD}}(t) \cong \alpha_{\text{skin DD}}(t), \tag{6}$$

we finally obtained

$$q(t) \cong \frac{\alpha_{\text{bone S-DD}}}{\alpha_{\text{bone S-PD}}} + \frac{\alpha_{\text{bone S}} \cdot \alpha_{\text{bone DD}}}{\alpha_{\text{bone S-PD}}} \alpha_{\text{SASS-DD}}(t). \tag{7}$$

For each and every measurement, the magnitude of this transillumination quotient (TQ) depends on: 1. the positions of the detectors, which are reflected in the constant coefficient $(\alpha_{\text{bone S}} \cdot \alpha_{\text{bone DD}})/\alpha_{\text{bone S-PD}}$ and background radiation $\alpha_{\text{bone S-DD}}/\alpha_{\text{bone S-PD}}$, and 2. instantaneous status (width) of the optical duct formed by the cerebrospinal fluid within the subarachnoid space, which is reflected in the time-dependent transmittance coefficients $\alpha_{\text{SAS S-DD}}(t)$.

As it appears, the TQ is almost completely independent of the very strong modulation introduced by pulsatile flow of blood within the skin of the head—elimination of proportional factors. With the prior assumptions, such elimination of proportional factors results from dividing the DD signal over that

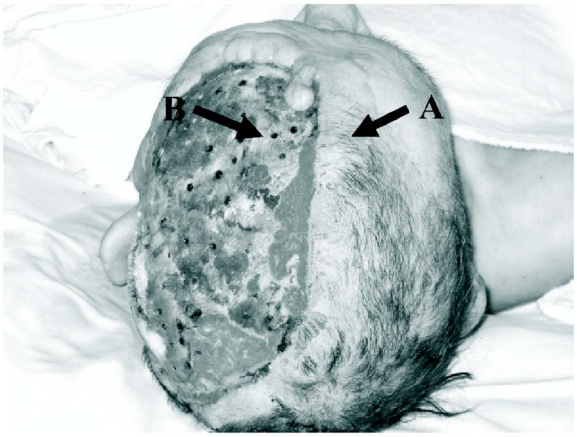

Fig. 3 Image of the head of the patient (age 57 years) who suffered from injury-induced scalp removal from the left half of the head. Photographed by Frydrychowski. Arrows point to the locations of the detectors (A and B). The protocol of the measurements was approved by the Independent Commission for Bioethics in Research at the Medical University of Gdańsk, approval number NKEBN/760/2002.

from the PD. Also, the depth of modulation (magnitude of instantaneous changes) of the TQ depends mainly on the propagation of NIR between the source and DD within the SAS.

3 Objective of the Study

The objective of this study was to verify the correctness of the assumptions assumed and calculations performed within the theoretical model, by comparing them with the results of real measurements of NIR-BSR with the method of NIR-T/BSS. For this verification, we utilized a very rare clinical case of a patient who was battered and lost her scalp from exactly one half of the head as a result of this injury (Fig. 3). With such conditions it became possible to compare the power of NIR-BSR using a detector placed on the surface of the skin of the head in the typical detector location at the level of the frontal tuber [Fig. 3(a)] with the power of NIR-BSR received by a detector located directly on the surface of the skull bone [Fig. 3(b)].

3.1 *Comparison of Results from Numerical Model with Real Measurement Data*

As already mentioned, such comparison was possible due to the availability of a the clinical case of patient with scalp removed from one half of the head, described before. The recordings of the powers of NIR-BSR acquired from the DD and PD are presented in Figs. 4 and 5.

Recording of the signals in the condition with scalp removed (left side, right windows) clearly reveals lack of pulsation of the signal from the left proximal detector (PD left), with only the noise of the receiver left. In the presence of scalp (right side, left windows), pulsation of the signal from the proximal detector (PD right) is evident, which means that NIR propagates longitudinally within the scalp and partly returns to the detector after reflection from the skull bone (apparent influence of the modulation introduced by pulsatile blood flow within the skin).

The amplitudes of the pulsatile signals recorded from the distal detectors on both sides of the head, whether the scalp is

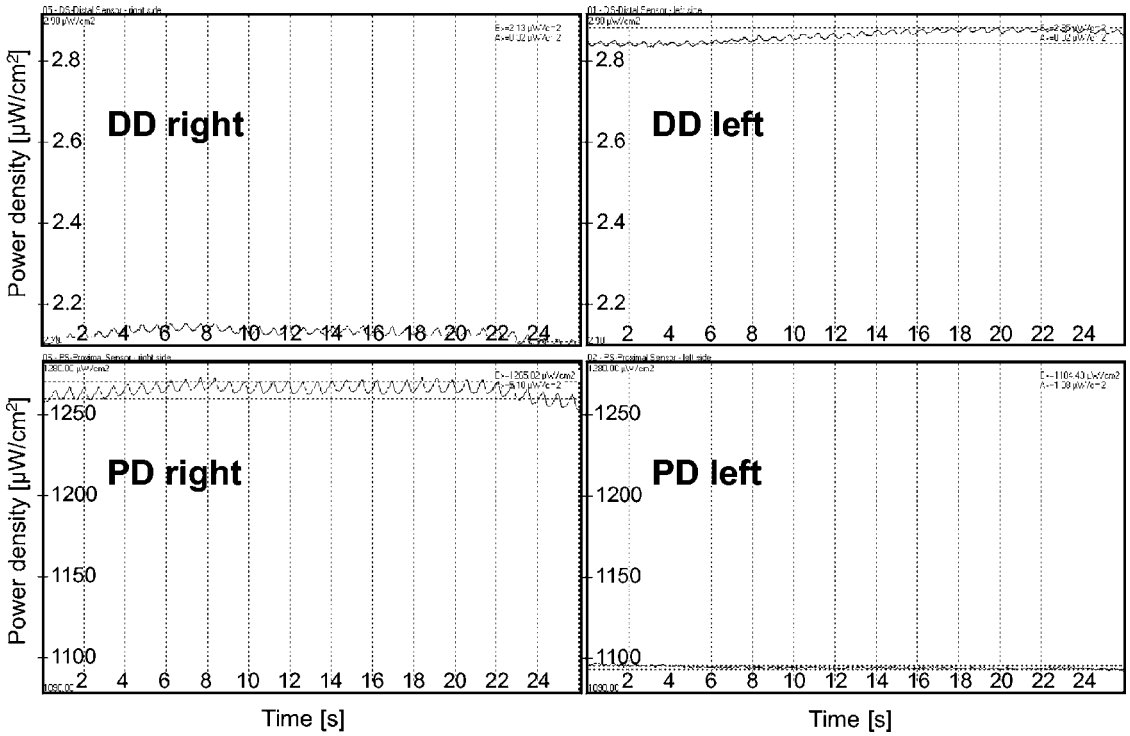

Fig. 4 Recordings of pulsatile NIR signals acquired from proximal detectors (PD) and distal detectors (DD) on both sides of the head of the patient. Comparison of the powers of the signals from the right and left PDs and DDs is possible, because the physical scales, in $\mu W/cm^2$ in vertical and in seconds in horizontal, are the same for all the signals.

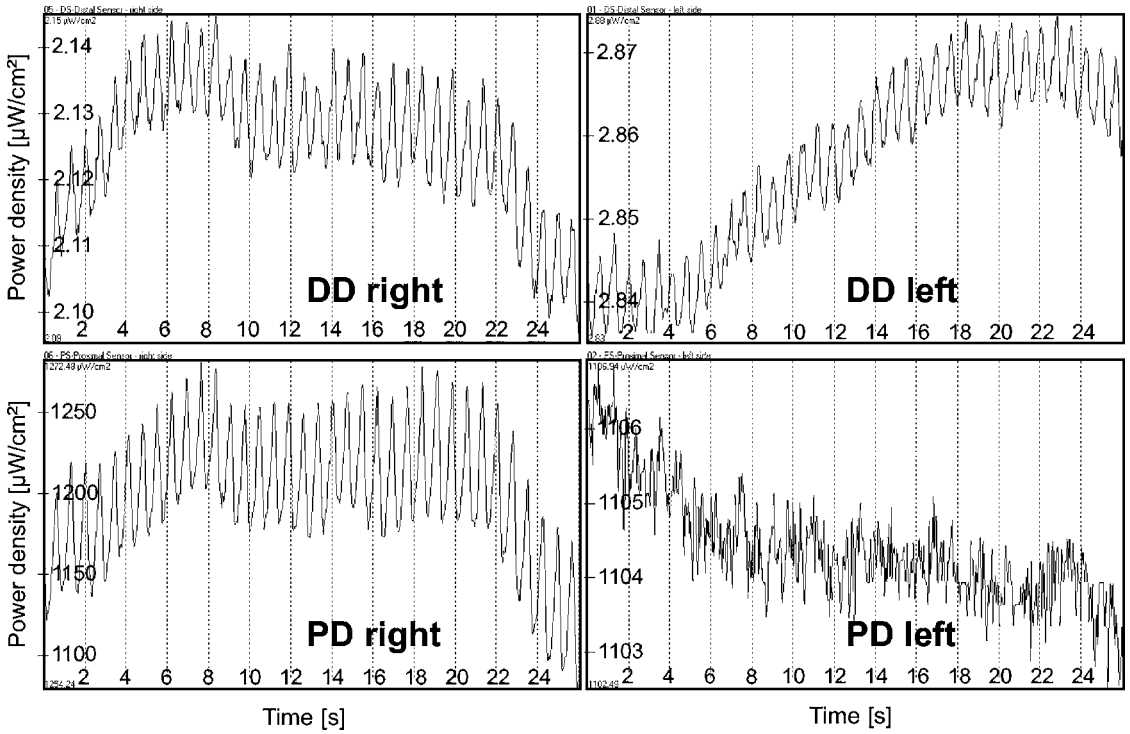

Fig. 5 Recordings of pulsatile NIR signals acquired from proximal detectors (PD) and distal detectors (DD) on both sides of the head of the patient. A best-fit scale yields maximum amplification of the waveforms at which they still fit their windows. Amplification is different for each waveform, but horizontal scales are the same.

present or not, are very similar, which confirms propagation of NIR between the source and DD within the SAS. The same observation also confirms the absence of longitudinal NIR propagation from the source to the DD within the skin (scalp) layer. Zero or near-zero amplitude of the signal acquired from the proximal detector placed directly on the skull bone indicates very small amplitude of pulsatile changes of the SAS width induced by cerebrovascular pulsation, while the much higher amplitude and distinct shape of the waveform of the signal from the PD placed on the surface of the scalp unequivocally suggests that the signal pulsation is due to modulation introduced by the pulsatile flow of blood within the scalp layer, as NIR propagates longitudinally within that layer, with only a minute fraction of the total NIR reflected back from the surface of the brain. Therefore, although NIR does not propagate longitudinally within the scalp from the source to the DD, it certainly does from the source to the PD.

Readings of intensity of NIR-BSR on the surface of the head, at the locations of the PD and DD, for source power 100 mW are presented in Table 1. The measured values are averaged signal intensities for each of the signals shown in the windows of Fig. 5. The calculated values were obtained with a Monte Carlo simulation procedure, whose results were presented in the first part of our study. In that simulation it was assumed that particular anatomical layers of the head are parallel; parameters of the layers used in the simulation are presented in Table 2. The data refer to the tissues of the particular patient in whom the transillumination measurements were performed. In particular, the thicknesses of the layers of the skull bone were measured on a piece of the bone planned for resection.

Both the results of real-life measurements and the output data from the numerical simulation of NIR propagation reveal very strong dependence of the intensity of the backscattered NIR on detector-source distance. Our results showed a 26- to 30 dB difference between the signals from the detector at a more proximal location with reference to the source (PD) and from that located farther away from the source (DD), regardless of the presence or absence of the scalp layer. The results indicate that the differences between the modeled and measured signal intensities are below 1.4 dB for the detector placed on the skin, and 4.5 dB for the detector placed directly on the skull bone, which is acceptable. On one hand, these differences depend on the accuracy of the optical parameters of the anatomical layers of the head, and the assumption that the thickness of those layers (particularly the skull bone and the SAS) is independent from their location within the head.

Table 1 Comparison of intensities of the backscattered NIR on the surface of the head.

	Detector	Calculated intensity [$\mu W/cm^2$]	Measured intensity [$\mu W/cm^2$]	Error [dB]
Detector placed on the scalp	PD	1734	1269	1.36
	DD	1.915	2.12	−0.44
Detector placed on the bone	PD	2981	1104	4.31
	DD	5.619	2.85	2.95

Table 2 Optical properties of tissues of the head used for numerical modeling.

Tissue	Thickness [mm]	Absorption coefficient μ_a[1/mm]	Reduced scattering coefficient μ_s'[1/mm]
Skin	3	0.013	1.7
Bone: external compact lamina	2	0.0242	0.88
Bone: spongious part	5	0.01627	0.59268
Bone: internal compact lamina	3	0.0242	0.88
SAS	0 to 5	0.001	0.001
Brain	10	0.037	2.0

On the other hand, they are affected by how tightly the detectors adhere to the surface of the head, especially with detector placement directly on the hard, nonflexible surface of the skull bone.

3.2 *Spectral Analysis*

The numerical model studies showed that the dependence of the intensity of backscattered NIR on the surface of the head on the width of the SAS is a nonlinear function. Changes of cerebrospinal fluid pulse pressure are correlated with the intracranial pressure,[15–17] which makes them dependent on the width of the SAS. Therefore, with a sinusoid cardiac-pumping-induced pattern of the changes of SAS width—an assumption that can be rightly made for the conditions of nonzero width of that space—we should expect higher-rank harmonics of the heart-rate frequency. The results of our measurements confirmed this expectation, as illustrated by Fig. 6.

In the case of our patient, nonzero width of the fluid-filled SAS was preserved. In patients with different types of craniocerebral pathology, momentary reductions of the width of the fluid layer to zero occur in the systolic phase, of each cardiac cycle, indicating early phases of cerebral edema. In such conditions we should expect much greater contributions to the power spectrum from higher-order harmonics. With the progression of cerebral edema, as more and more fluid from the cranial compartment of the SAS is displaced into the spinal compartment and SAS width eventually is completely exhausted, it would be logical to expect the disappearance of both the fundamental and higher harmonics. Analysis of the distribution of harmonics within the spectrum can provide grounds for estimation of the progression and tendency of cerebral edema. Elaboration of more precisely defined criteria for such estimations requires further studies on real patients with cerebral edema of different degrees.

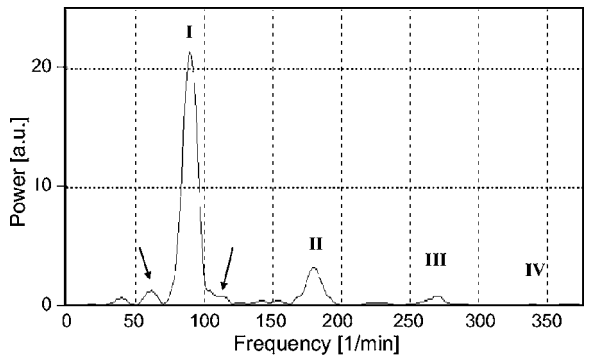

Fig. 6 Power spectrum of the waveform of transillumination quotient (TQ) for the SAS. Fundamental frequency (or first cardiac harmonic, I) equal to heart rate, II second harmonic, III third harmonic, and IV fourth harmonic. Small amplitude peaks below and above the fundamental frequency (marked with arrows) are caused by the natural phenomenon of respiratory sinus arrhythmia.

4 Discussion

The results obtained within this study indicate that, given appropriate design and manufacturing of the source-detector module, it is possible to record changes in the width of the SAS with use of near-infrared radiation. The magnitude of the changes in the amount of radiation propagated in time from the NIR source to a detector placed on the surface of the skin of the head depends on both SAS width and source-detector distance.

The output data presented in part one of our research demonstrated that, with source-detector distance exceeding 6 mm, the contribution of the radiation propagated longitudinally within the skin only to the overall radiation received by the detector is negligible. However, NIR is considerably attenuated within the skin, and the absolute power of the radiation received by the detector is therefore strongly affected by the optical properties of the skin (Fig. 4). This influence of the skin may be the cause of some, however minor (2 to 4 dB), discrepancies between the results of numerical modeling and those of real measurements in human subjects.

With relatively small source-detector distance (within the range 5 to 20 mm, depending on the thickness of skull bone), the power of optical radiation reaching the detector after being propagated within the deeper tissue layers, i.e., within the SAS, is too low compared with that of radiation propagated within more superficial layers, i.e., scalp only or scalp and bone only). In such conditions, when the detector is located close to the NIR source, recording of the changes in the width of the SAS based on the analysis of changes in the power of NIR received by the detector is not possible.

Our results show that relative changes of the received optical signal resulting from the fluctuations of the width of the SAS depend on the source-detector distance. If that distance is too low (below 15 mm), the power of radiation received by the detector remains constant within the full analyzed range of SAS width. Contrary to this, as source-detector distance increases above 15 mm, a progressive increase of relative changes of the received signal in the function of SAS width is observed. This dependence can be attributed to the presence of a specific biological optical duct, constituted by the SAS—the space between the skull bone and the surface of the brain, filled with water-clear cerebrospinal fluid. Properties of this duct influence changes in the intensity of the optical radiation propagated therein, due to multiple reflections and scattering occurring between the inner surface of the skull bone and the

surface of the brain. An increase in the width of the SAS allows for more photons of NIR to reach the detector, which results in an increase of the intensity of the received signal; whereas a decrease in SAS width causes a decrease of the power of the radiation reaching the detector.

These observations lead us to the conclusion that, with the detector positioned far enough from the NIR source, it is possible to measure changes in the power of radiation propagated within the optical duct formed by the SAS. Noteworthy is the fact that the power of the received radiation and the width of the SAS were found to be distinctly convergent. The collected data that describe the influence of source-detector distance on the level of power of the received signal are also consistent with the results of studies on that dependence done by other authors.[18–23]

For successful construction of a SAS-width measurement system, it is very important to have the information on relative changes of the power of the radiation received by the detector, in the function of source-detector distance, for a given SAS width. The results of numerical modeling and precise calculations of the optimum positions for each of the detectors enabled the design and manufacturing of a set of dedicated source-detector modules to be used for the monitoring of the changes in SAS width in patients.

Theoretical considerations and real-life recordings with NIR-T/BSS presented here proved that the method of near-infrared transillumination may win a number of clinical applications in such fields as: 1. intensive neurological care (e.g., stroke patients), 2. traumatology (craniocerebral injuries, detection of early phases of cerebral edema or monitoring of the effectiveness of the applied treatment), 3. screening for significant asymmetry in cerebrovascular pulsation as indication for targeted CT scans or other neuroimaging techniques, 4. preliminary detection of signs of craniocerebral injury in unconscious patients (e.g., ones with ethanol intoxication), 5. evaluation of the effectiveness of treatment with vasoactive agents, 6. monitoring of cerebrovascular pulsation during carotid endarterectomy aimed at assessment of collateral circulation and detection of potential postsurgery hyperperfusion, 7. objective assessment of the vasoactive component of different types of headaches cerebrovascular constriction or dilation, 8. neurosurgery—monitoring of patients with intracranial hematomas, elevated intracranial pressure, or brain tumours, 9. psychiatry—monitoring of cerebrovascular function during and after electroconvulsive therapy, 10. cardiac surgery—monitoring of intracranial homeostasis, e.g., in patients subjected to coronary artery by-pass grafting (CABG), with use of extracorporeal circulation, 11. monitoring of cerebrovascular pulsation in patients undergoing any type of surgery likely to cause impairment of cerebral blood supply, and 12. monitoring changes in SAS width and parameters of cerebrovascular pulsation.

Another great value of the NIR-T/BSS method is that it is totally safe and noninvasive for both the patient and medical personnel. It also does not affect in any way the physiological regulatory mechanisms controlling the variables under investigation. It is important that the hardware of the NIR-T/BSS system does not generate any signals that could interfere with other diagnostic or therapeutic equipment used in patient management.

For potential clinical application of this method, it is also valuable that: 1. the ease of use of the system allows for its employment in almost any clinical conditions, including intraoperative or bedside monitoring, 2. the system is capable of recording the signals over a prolonged period of time, which makes this method suitable for monitoring of the changes in SAS width and magnitude of cerebrovascular pulsation, and 3. the method is equipped with advanced and versatile software, which enables a number of on-line analyses of the recorded waveforms.

The results that we obtained earlier in other patients also suggest that the use of NIR-T/BSS in patients with head injuries may contribute to optimization of the use of computerized tomography (CT) scans or magnetic resonance imaging (MRI) by: 1. indicating important instants where such examinations could be particularly informative and thus increasing patient safety, and 2. preventing unnecessary use of these diagnostic techniques when there are no dynamic changes observed with NIR-T/BSS, thus reducing the related burden for the patient and cost for the healthcare system.

Last but not least, in comparison to other diagnostic methods, NIR-T/BSS is a very low-cost modality, with no hidden extra costs involved.

References

1. J. Pluciński, A. F. Frydrychowski, J. Kaczmarek, and W. Juzwa, "Theoretical foundations for noninvasive measurement of variations in the width of the subarachnoid space," *J. Biomed. Opt.* **5**(3), 291–306 (2003).
2. J. Pluciński and A. F. Frydrychowski, "Verification with numeric modeling of optical measurement of changes in the width of the subarachnoid space," *Biocyber. Biomed. Eng.* **19**(4), 111–126 (1999).
3. A. F. Frydrychowski, W. Gumiński, M. Rojewski, J. Kaczmarek, and W. Juzwa, "Technical foundation for non-invasive assessment of changes in the width of the subarachnoid space with near-infrared transillumination-back scattering sounding (NIR-TBSS)," *IEEE Trans. Biomed. Eng.* **49**(8), 887–904 (2002).
4. A. F. Frydrychowski, "Subarachnoidal space monitoring system," World Intellectual Property Organization WO 96/25876, PCT/PL95/00018, Geneva (1995).
5. A. F. Frydrychowski, "NIR-T/BSS near-infrared transillumination with back-scattering sounding (NIR-T/BSS): a new, noninvasive method of assessment of the width of the subarachnoid space and parameters of cerebrovascular pulsation," *Ann. Acad. Med. Gedanensis* **35**(7) (2005).
6. A. F. Frydrychowski, J. Kaczmarek, W. Juzwa, M. Rojewski, J. Pluciński, W. Gumiński, Cz. Kwiatkowski, P. Lass, and T. Bandurski, "Near-infrared-transillumination (NIR-TI)—a new non-invasive tool for exploration of intracranial homeostasis and monitoring of its impairments," *Biocyber. Biomed. Eng.* **19**(2), 99–108 (1999).
7. A. F. Frydrychowski, W. Gumiński, J. Kaczmarek, P. Lass, M. Rojewski, W. Juzwa, and T. Bandurski, "Detection of hypercapnia-induced changes in amplitude of cerebrovascular pulsation in humans with non-invasive technique of near-infrared transillumination," *J. Physiol. Pharmacol.* **50**(1), 138 (1999).
8. A. F. Frydrychowski, M. Rojewski, W. Gumiński, J. Kaczmarek, and W. Juzwa, "Aplication of transilluminatuion quotient for monitoring of the instantaneous width of the subarachnoid space," *Opto-Electron. Rev.* **9**(4), 403–411 (2001).
9. A. F. Frydrychowski, M. Rojewski, W. Gumiński, J. Kaczmarek, and W. Juzwa, "Near infrared transillumination-back scattering (NIRT-BS)—a new method for non-invasive monitoring of changes in width of subarachnoid space and magnitude of cerebrovascular pulsation," *Opto-Electron. Rev.* **9**(4), 397–402 (2001).
10. A. F. Frydrychowski, M. Rojewski, and W. Gumiński, "Spectral analysis of mechanical and respiratory influences on width of subarachnoid space assessed with non-invasive method of near-infrared transillumination/back scattering sounding," *Opto-Electron. Rev.* **10**(2), 151–157 (2002).

11. A. F. Frydrychowski, M. Rojewski, and W. Gumiński, "Monitoring of subarachnoid space and cerebrovascular pulsation with near-infrared transillumination/back scattering—new aspects of the method," *Opto-Electron. Rev.* **10**(3), 175–184 (2002).
12. P. W. McCormick, M. Stewart, M. Dujovny, and J. I. Ausman, "Clinical application of diffuse near infrared transmission spectroscopy to measure cerebral oxygen metabolism," *Hospimedica* **8**(4), 39–47 (1990).
13. P. W. McCormick, M. Stewart, M. G. Goetting, M. Dujovny, G. Lewis, and J. I. Ausman, "Noninvasive cerebral optical spectroscopy for monitoring cerebral oxygen delivery and homodynamic," *Crit. Care Med.* **19**, 89–97 (1991).
14. P. Smielewski, P. Kirkpatrick, P. Minhas, J. D. Pickard, and M. Czosnyka, "Can cerebrovascular reactivity be measured with near-infrared spectroscopy?" *Stroke* **26**, 2285–2292 (1995).
15. P. H. Klose, G. D. Lewis, W. P. Messing, R. R. Kasperski, and J. M. Flemming, "Noninvasive infrared cerebral oximetry," *Proc. SPIE* **1641**, 202–207 (1992).
16. C. J. J. Avezaat and J. H. M. Eijndhoven, "Clinical observations on the relationship between cerebrospinal fluid pulse pressure and intracranial pressure," *Acta Neurochir.* **79**(1), 13–29 (1986).
17. C. J. J. Avezaat, J. H. M. Eijndhoven, and D. J. Wyper, "Cerebrospinal fluid pulse pressure and intracranial volume-pressure relationship," *J. Neurol., Neurosurg. Psychiatry* **42**, 687–700 (1979).
18. E. Okada, M. Firbank, M. Schweiger, S. R. Arridge, M. Cope, and D. T. Delpy, "Theoretical and experimental investigation of near-infrared light propagation in a model of the adult head," *Appl. Opt.* **36**(1), 21–31 (1997).
19. E. Okada, M. Saito, M. Firbank, and D. T. Delpy, "Monte Carlo investigation of the effect of skull optical properties on optical pathlength in the brain," *Proc. SPIE* **3194**, 28–33 (1998).
20. E. Okada and D. T. Delpy, "Near infrared light propagation in adult head model. I. Modeling of low-level scattering in the cerebrospinal fluid layer," *Appl. Opt.* **42**(16), 2906–2914 (2003).
21. E. Okada and D. T. Delpy, "Near infrared light propagation in an adult head model. II. Effect of superficial tissue thiskness on the sensitivity of the near-infrared spectroscopy signal," *Appl. Opt.* **42**(16), 2925–2922 (2003).
22. S. L. Jacques, A. Gutsche, J. Schwartz, L. Wang, and F. Tittel, "Video reflectometry to specify optical properties of tissue in vivo, in medical optical tomography: functional imaging and monitoring," *Proc. SPIE* **IS11**, 211–226 (1993).
23. S. L. Jacques, "Tissue optics," short course notes SC01, SPIE Press, Bellingham, WA (1997).